J. Fluid Mech. (1990), *vol.* 215, *pp.* 85–100
Printed in Great Britain

Frequency response of electrochemical sensors to hydrodynamic fluctuations

By C. DESLOUIS, O. GIL AND B. TRIBOLLET

LP15 du CNRS Physique des Liquides et Electrochimie, Laboratoire de l'Université Pierre et Marie Curie, Tour 22, 4 place Jussieu, 75252 Paris Cedex 05, France

(Received 4 October 1988 and in revised form 23 October 1989)

The response of mass transfer to a small mass sink to hydrodynamic fluctuations in the concentration boundary layer has been calculated as a function of frequency. The dimensionless local flux was expressed as a series expansion of the dimensionless local diffusion layer thickness η and the dimensionless local characteristic frequency ξ in the low frequency range, and as the asymptotic power law $\xi^{-\frac{3}{2}}$, in the high frequency range. The two solutions were shown to overlap fairly well for $6 \leqslant \xi \leqslant 13$. The overall transfer function over the whole mass sink area involves a spatial distribution for which the low-frequency approximation applies at the upstream end and the high-frequency approximation applies downstream. The average response at frequency f varies as f^{-1}

These theoretical predictions were tested electrochemically by using a rotating disk. The modulated limiting diffusion current due to a fast redox reaction at small circular microelectrodes embedded in the disk was measured as a function of the frequency of the modulation of the disk angular velocity.

1. Introduction

The wall shear stress τ_w or the velocity gradient α at the wall are widely measured electrochemically using the diffusion current I given by a redox reaction:

$$\alpha = \frac{\tau_w}{\mu} = AI^3, \tag{1}$$

where μ is the viscosity and A depends on the probe dimensions, active species concentration and solution temperature. Relation (1) is valid only in steady-state conditions.

When α is time dependent, the current $I(t)$ is defined by the convolution product:

$$I(t) = h(t) * \alpha(t), \tag{2}$$

where $h(t)$ is the impulse response of the system.

An analysis in the time domain to deduce $\alpha(t)$ from $I(t)$ is easy only for quasi-steady-state conditions (i.e. for large structures associated with low frequencies in turbulent flows) or for fully developed laminar periodic flows such as, e.g. those occurring in blood circulation (Patel, McFeely & Jolls 1975). In this last case, the instantaneous wall velocity gradient $\alpha(t)$ can be deduced from the instantaneous diffusion current $I(t)$, if $h(t)$, or its complex Fourier transform $\mathscr{H}(f)$, are known.

In contrast, a spectrum analysis in the frequency domain is easier for investigating turbulence or unstable systems: This requires dealing with a linear theory, which

implies that the level of the velocity perturbations is locally (i.e. in the diffusion layer) much smaller than the mean flow velocity at any frequency.

It has been shown that the power spectral density (p.s.d.) W_I of the diffusion current fluctuations is linked to the p.s.d. of the velocity gradient fluctuations W_α through the relationship (Deslouis, Tribollet & Viet 1983; Nakoryakov, Kashinsky & Kozmenko 1983):

$$W_I = |\mathscr{H}(f)|^2 W_\alpha, \tag{3}$$

where $\mathscr{H}(f)$ is the transfer function of the diffusion current response of a microelectrode to a sinusoidal modulation of a steady flow.

For turbulence investigations, the p.s.d. of the diffusion current fluctuations W_I is experimentally measured, and the velocity gradient spectrum W_α is deduced by applying (3), and therefore only the amplitude $|\mathscr{H}(f)|$ is needed.

In the past, the use of electrochemical sensors was restricted to the quasi-steady-state domain for which $|\mathscr{H}(f)|$ is constant. Since the associated cutoff frequency is rather low owing to a high Schmidt number value in liquids ($Sc = \nu/D \approx 10^3$), such a procedure considerably limited the usefulness of mass transfer sensors. If the transfer function is accurately determined at high frequencies, it is possible using (3) to analyse fluctuations of the wall velocity gradient over a wide frequency range. This will make mass transfer sensors as attractive as thermal sensors (e.g. hot wires).

It is not our purpose to give an exhaustive account of all the theoretical works, either by numerical or analytical techniques, devoted to the calculation of this transfer function at any frequency.

Most of the authors (see Bogolyugov *et al.* 1972; Dumaine 1981; Vorotyntsev, Martem'Yanov & Grafov 1984; Ambari, Deslouis & Tribollet 1986) found an asymptotic behaviour of $|\mathscr{H}(f)|$ at large frequencies as a power law $f^{-\frac{3}{2}}$ for a circular or rectangular sensor. Fortuna & Hanratty (1971) proposed the same frequency dependence for the local mass transfer rate.

Mao & Hanratty 1985, again by a numerical technique, found a variation of $|\mathscr{H}(f)|$ proportional to f^{-1} in the high frequency range and a limiting phase shift equal to $-90°$. At the same time, Nakoryakov *et al.* 1986, obtained from a numerical integration an expression of $\mathscr{H}(f)$ in the whole frequency range, which presents a high-frequency asymptotic behaviour in agreement with the recent data of Mao & Hanratty (1985).

In contrast to these theoretical studies, as mentioned by Talbot & Steinert (1987), there is a lack of detailed experimental studies of the frequency response (with respect to both amplitude and phase) of local electrochemical mass transfer shear probes under controlled conditions where the correct amplitude and phase are accurately known. This experimental problem is due to the difficulty of getting a very well defined periodic flow in a pipe or channel. So, up to now, no conclusive and quantitative verification of $\mathscr{H}(f)$ calculations (both in amplitude and phase) has been given.

In this work, we aimed first at deriving an accurate analytical expression for $\mathscr{H}(f)$, valid for rectangular or circular probes. Comparison with the previous expressions will help to understand some of the apparent discrepancies between the different works listed as references.

Secondly, accurate experimental verification of this calculation will be given from the diffusion current measurement on a circular probe embedded in a rotating disk. The flow generated by a rotating disk is well known and presents some particular advantages for this problem: the Navier–Stokes equations had been solved for the steady flow by Kármán (1921) and Cochran (1934), and for the unsteady flow by

Tribollet & Newman (1983), and a well-defined periodic flow can be easily obtained simply by modulating sinusoidally the disk speed around a mean value. Hence, electrochemical probes of defined geometry are now very well suited for determining the instantaneous velocity gradient in periodic flows or for deducing the p.s.d. of velocity gradients in turbulent or unsteady flows from mass transfer fluctuations measurements.

2. Statement of the problem

We consider a rectangular probe with its long side perpendicular to the direction of the mean flow or a circular probe, both embedded flush with a solid wall. The length l of the rectangular element in the mean flow direction or the diameter d of the circular one are small enough to neglect the effect of the normal velocity component as analysed by Mollet *et al.* (1974).

If the width L of a rectangular probe is large enough, the edge effects in the transverse direction (coordinate z) are negligible, and therefore the first two derivatives of the concentration $\partial c/\partial z$ and $\partial^2 c/\partial z^2$ can be neglected. For a circular probe the dimensions in the x- and z-directions are the same, and in principle $\partial c/\partial z$ and $\partial^2 c/\partial z^2$ cannot be *a priori* neglected.

In addition, we consider situations such that $\bar{\alpha} l^2/D$ or $\bar{\alpha} d^2/D$ is larger than 5000 in order to neglect diffusion in the direction of the mean flow (coordinate x) as shown by Ling (1963). Owing to the above mentioned fact that the dimensions in the x- and z-directions are the same for a circular probe, we assume that both $\partial^2 c/\partial z^2$ and $\partial^2 c/\partial x^2$ can be neglected.

3. Frequency response of the transient local mass flux

In boundary-layer approximation, the mass balance equation governing the concentration distribution c of a species transported by convection and diffusion is:

$$\frac{\partial c}{\partial t} + \alpha y \frac{\partial c}{\partial x} + \beta y \frac{\partial c}{\partial z} = D \frac{\partial^2 c}{\partial y^2}, \tag{4}$$

where $V_x = \alpha y$, $V_z = \beta y$ with $\bar{\beta} = 0$, since there is no mean flow in the transverse direction. The overbar designates a time average value.

For simplification, we consider that the electrochemical sensor fulfils the homogeneity condition, or in other words, is sufficiently small that any flow modulation is uniform in space over the sensor at any instant: then α and β are assumed independent of the space coordinates.

For both geometries, the time-average solution of Leveque (1928) is valid:

$$\bar{c} = \frac{c_\infty}{3^{\frac{2}{3}}\Gamma(\frac{4}{3})} \int_0^{y/\delta(x,z)} \exp(-\tfrac{1}{9}\eta^3)\, \mathrm{d}\eta, \tag{5}$$

where c_∞ is the species concentration in the bulk and $\delta(x,z) = [(D/\bar{\alpha}(x - x_1(z))]^{\frac{1}{3}}$. The local value of the diffusion layer thickness is $3^{\frac{2}{3}}\Gamma(\frac{4}{3})$ times $\delta(x,z)$. $x_1(z)$ represents the position of the leading edge of the probe with the conventions of figure 1.

$$x_1(z) = R - (R^2 - z^2)^{\frac{1}{2}} \quad \text{for a circular probe.}$$

$$x_1(z) = 0 \quad \text{for a rectangular probe.}$$

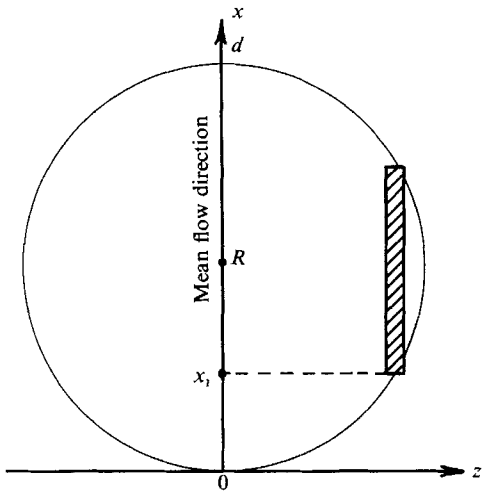

FIGURE 1. Scheme of the circular microelectrode.

On a rectangular or a circular probe the steady-state flux is respectively:

$$\bar{J}_{\mathrm{R}} = L\int_0^l D\frac{\partial \bar{c}}{\partial y}\mathrm{d}x = \frac{3^{\frac{1}{3}}c_\infty D^{\frac{2}{3}}\bar{\alpha}^{\frac{1}{3}}l^{\frac{2}{3}}L}{2\Gamma(\frac{4}{3})}, \tag{6}$$

$$\bar{J}_{\mathrm{c}} = \int_{-R}^{R}\mathrm{d}z\int_{R-(R^2-z^2)^{\frac{1}{2}}}^{R+(R^2-z^2)^{\frac{1}{2}}} D\frac{\partial \bar{c}}{\partial y}\mathrm{d}x = 0.84\frac{3^{\frac{1}{3}}c_\infty D^{\frac{2}{3}}\bar{\alpha}^{\frac{1}{3}}d^{\frac{5}{3}}}{2\Gamma(\frac{4}{3})}. \tag{7}$$

We consider a modulated flow such that:

$$V_x = \bar{\alpha}y + \mathrm{Re}\{\tilde{\alpha}y\exp \mathrm{i}\omega t\}, \tag{8}$$

$$V_z = \mathrm{Re}\{\tilde{\beta}y\exp \mathrm{i}\omega t\}. \tag{9}$$

Re means the real part and the symbol $\sim$ represents a complex quantity.

The instantaneous concentration distribution is thus defined as

$$c = \bar{c} + \mathrm{Re}\{\tilde{c}\exp \mathrm{i}\omega t\}. \tag{10}$$

The hydrodynamic perturbation must be small enough for minimizing the quadratic terms ($\tilde{\alpha}(\partial\tilde{c}/\partial x)$ and $\tilde{\beta}(\partial\tilde{c}/\partial z)$) and therefore for satisfying the linearity conditions. These conditions can be written as $|\tilde{\alpha}/\bar{\alpha}| \ll 1$ and $\partial\tilde{c}/\partial z \ll \partial\bar{c}/\partial z$. This calculation is therefore consistent with the assumption of a linear theory of the turbulent fluctuations. Then, the non-steady part of the mass balance equation may be written as

$$\mathrm{i}\omega\tilde{c} - D\frac{\partial^2\tilde{c}}{\partial y^2} + y\bar{\alpha}\frac{\partial\tilde{c}}{\partial x} = -y\tilde{\alpha}\frac{\partial\bar{c}}{\partial x} - y\tilde{\beta}\frac{\partial\bar{c}}{\partial z}. \tag{11}$$

The boundary conditions for the steady-state and non-steady-state equations are

$$\tilde{c}, \bar{c} = 0 \quad \text{for } y = 0, x \geqslant x_1,$$

$$\frac{\partial\bar{c}}{\partial y}, \frac{\partial\tilde{c}}{\partial y} = 0 \quad \text{for } y = 0, x < x_1,$$

$$\bar{c} = \bar{c}_\infty, \quad \tilde{c} = 0 \quad \text{for } y \to \infty.$$

The form of (11) suggests, as proposed by Nakoryakov *et al.* (1986), introducing the dimensionless function h using

$$\tilde{c} = c_\infty \left(\frac{\tilde{\alpha}}{\bar{\alpha}} - \frac{\mathrm{d}x_1}{\mathrm{d}z} \frac{\tilde{\beta}}{\bar{\alpha}} \right) h, \tag{12}$$

and the dimensionless variables

$$\eta = y \left(\frac{\bar{\alpha}}{D(x-x_1)} \right)^{\frac{1}{3}}, \quad \xi = \omega \left(\frac{(x-x_1)^2}{D\bar{\alpha}} \right)^{\frac{1}{3}},$$

which correspond to $\eta = y/\delta$ and $\xi = \omega\delta^2(x)/D$.

Equation (11) then becomes:

$$\mathrm{i}\xi h + \tfrac{2}{3}\xi\eta \frac{\partial h}{\partial \xi} - \tfrac{1}{3}\eta^2 \frac{\partial h}{\partial \eta} - \frac{\partial^2 h}{\partial \eta^2} = \frac{\eta^2 \exp(-\frac{1}{9}\eta^3)}{3^{\frac{5}{3}}\Gamma(\frac{4}{3})}. \tag{13}$$

3.1. *Low-frequency solution (quasi steady state)*

As suggested by Pedley (1972) and Nakoryakov *et al.* (1986) we seek a solution in the form:

$$h = \sum_{m=0}^{\infty} (\mathrm{i}\xi)^m h_m(\eta). \tag{14}$$

The elementary functions $h_m(\eta)$ are real and obey the equations:

$$\frac{\mathrm{d}^2 h_0}{\mathrm{d}\eta^2} + \tfrac{1}{3}\eta^2 \frac{\mathrm{d}h_0}{\mathrm{d}\eta} = \frac{-\eta^2 \exp(-\frac{1}{9}\eta^3)}{3^{\frac{5}{3}}\Gamma(\frac{4}{3})}, \tag{15}$$

$$\frac{\mathrm{d}^2 h_m}{\mathrm{d}\eta^2} + \frac{\eta^2}{3}\frac{\mathrm{d}h_m}{\mathrm{d}\eta} - \tfrac{2}{3}m\eta h_m = h_{m-1} \quad \text{for } m = 1, 2, \ldots. \tag{16}$$

$h_0(\eta)$ is readily obtained analytically

$$h_0(\eta) = \frac{\eta \exp(-\frac{1}{9}\eta^3)}{3^{\frac{5}{3}}\Gamma(\frac{4}{3})}, \quad \left.\frac{\mathrm{d}h_0}{\mathrm{d}\eta}\right|_0 = \frac{1}{3^{\frac{5}{3}}\Gamma(\frac{4}{3})}.$$

After the boundary conditions of (11) one has $\tilde{c}(\eta = 0) = 0$, then $h(\eta = 0) = 0$ and hence $h_m(\eta = 0) = 0$ for any m.

In fact, since only the interface flux is the observable quantity, we need only to know the $\partial h/\partial\eta\,|_0$ expression:

$$\left.\frac{\partial h}{\partial \eta}\right|_0 = \sum_{m=0}^{\infty} (\mathrm{i}\xi)^m \left.\frac{\partial h_m}{\partial \eta}\right|_0. \tag{17}$$

By using Newman's method of integration of partial differential equations (Newman 1968), we calculated the functions $h_m(\eta)$ and deduced the derivatives of first order at $\eta = 0$. Those values are listed in table 1 for $m \leqslant 59$. One question arises about the required number of terms to be retained in the expansion of (17) and the relevant convergence radius of the series. $(\partial h_m/\partial\eta)|_0$ values in table 1 indicate that the series is alternate and therefore convergent if beyond a certain rank n one has $|u_n/u_{n+1}| > 1$, i.e. here

$$\left| \frac{\left.\frac{\partial h_n}{\partial \eta}\right|_0}{\left.\frac{\partial h_{n+1}}{\partial \eta}\right|_0} \right| > 1.$$

m	$\left.\frac{\partial h_m}{\partial \eta}\right\|_0$	m	$\left.\frac{\partial h_m}{\partial \eta}\right\|_0$	m	$\left.\frac{\partial h_m}{\partial \eta}\right\|_0$	m	$\left.\frac{\partial h_m}{\partial \eta}\right\|_0$
0	0.179455	15	-0.318475×10^{-12}	30	0.174455×10^{-29}	45	-0.535893×10^{-49}
1	-0.991917×10^{-1}	16	0.284021×10^{-13}	31	-0.996095×10^{-31}	46	0.234787×10^{-50}
2	0.354269×10^{-1}	17	-0.243116×10^{-14}	32	0.556741×10^{-32}	47	-0.101393×10^{-51}
3	-0.975289×10^{-2}	18	0.200214×10^{-15}	33	-0.304809×10^{-33}	48	0.431734×10^{-53}
4	0.222240×10^{-3}	19	-0.158969×10^{-16}	34	0.163567×10^{-34}	49	-0.181310×10^{-54}
5	-0.436312×10^{-3}	20	0.121925×10^{-17}	35	-0.860814×10^{-36}	50	0.751192×10^{-56}
6	0.757506×10^{-4}	21	-0.904844×10^{-19}	36	0.444539×10^{-37}	51	-0.307127×10^{-57}
7	-0.118465×10^{-4}	22	0.650776×10^{-20}	37	-0.225384×10^{-38}	52	0.123947×10^{-58}
8	0.169190×10^{-5}	23	-0.454232×10^{-21}	38	0.112244×10^{-39}	53	-0.493868×10^{-60}
9	-0.223024×10^{-6}	24	0.308086×10^{-22}	39	-0.549334×10^{-41}	54	0.194334×10^{-61}
10	0.273645×10^{-7}	25	-0.203295×10^{-23}	40	0.264321×10^{-42}	55	-0.755356×10^{-63}
11	-0.314680×10^{-8}	26	0.130652×10^{-24}	41	-0.125093×10^{-43}	56	0.290077×10^{-64}
12	0.341839×10^{-9}	27	-0.818606×10^{-26}	42	0.582529×10^{-45}	57	-0.110085×10^{-65}
13	-0.350156×10^{-10}	28	0.500506×10^{-27}	43	-0.267023×10^{-46}	58	0.412938×10^{-67}
14	0.341839×10^{-11}	29	-0.298879×10^{-28}	44	0.120527×10^{-47}	59	-0.153134×10^{-68}

TABLE 1. Coefficients of the series expansion of equation (17)

	From Nakoryakov *et al.* (1986)		From (17)			From (21)	
ξ	Re	Im	Re	Im	m_{max}	Re	Im
0	0.1795	0	0.1795	0	1	—	—
1	0.1461	−0.0899	0.1462	−0.0899	9	—	—
2	0.0688	−0.1328	0.0689	−0.1329	12	—	—
3	−0.0049	−0.1181	−0.0049	−0.1182	16	—	—
4	−0.0416	−0.07261	−0.0416	−0.0726	21	—	—
5	−0.0411	−0.0315	−0.0411	−0.0314	24	—	—
6	−0.0248	−0.0117	−0.0247	−0.0117	28	—	—
7	−0.0117	−0.0089	−0.0116	−0.0090	33	−0.0137	−0.0137
8	−0.0072	−0.0114	−0.0072	−0.0115	38	−0.0112	−0.0112
9	−0.0076	−0.0120	−0.0076	−0.0121	44	−0.0094	−0.0094
10	−0.0083	−0.0101	−0.0084	−0.0102	51	−0.0080	−0.0080
11	−0.0078	−0.0078	−0.0078	−0.0078	57	−0.0069	−0.0069
12	−0.0066	−0.0062	−0.0065	−0.0063	66	−0.0061	−0.0061
13	−0.0055	−0.0053	−0.0051	−0.0052	73	−0.0054	−0.0054

TABLE 2. Dependence of the dimensionless local flux $\mathrm{d}h/\mathrm{d}\eta|_0$ on the dimensionless frequency ξ

The ratio between the two following terms of ranks n and $n+1$ in table 1 is approximated by

$$\frac{\left.\frac{\partial h_n}{\partial \eta}\right|_0}{\left.\frac{\partial h_{n+1}}{\partial \eta}\right|_0} = -1.776\,(n+1)^{\frac{2}{3}}. \tag{18}$$

Therefore, the series is convergent for any ξ value provided that a sufficiently high number of terms is used. However, one must consider that for mid or high ξ values, the first terms of the series are increasing up to a rank n such that $n \approx (\xi/1.776)^{\frac{3}{2}}-1$, and beyond, they are decreasing. Each of these first terms can have very high values

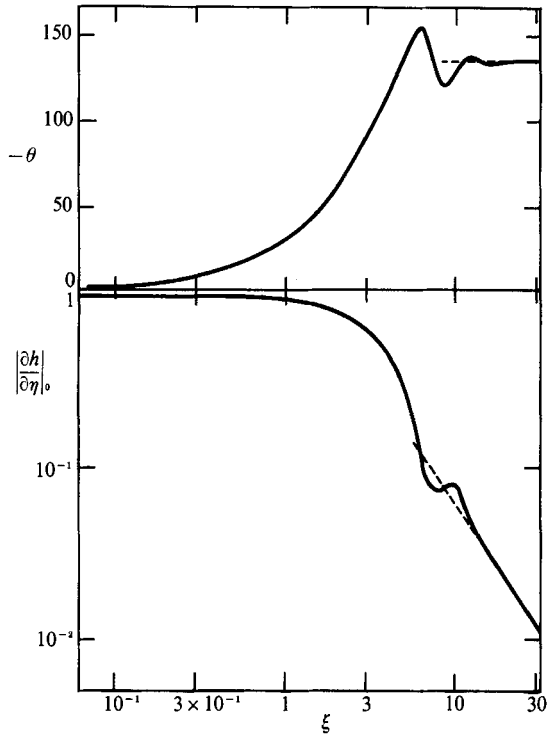

FIGURE 2. Dimensionless flux $\partial h/\partial\eta|_0$ *vs.* ξ showing overlap of (17) and (21).

though we will show further that the sum becomes very small at high ξ values. This requires that not only a sufficient number of terms is considered but also that each term is expressed with a number of significant figures which increases with ξ.

As an illustration, table 2 reports a comparison between the value of the sum of the series given by (17) in real and imaginary parts as determined by our technique and that obtained by Nakoryakov *et al.* (1986) from a direct numerical integration.

Also mentioned in table 2 is the number of terms needed ($m_{\max}$ column) in the series in order to get a satisfactory convergence for the ξ value considered. The terms of rank larger than 59 are deduced from $\mathrm{d}h_{59}/\mathrm{d}\eta|_0$ by the expression (18).

3.2. *High-frequency solution. Asymptotic behaviour*

The high-frequency solution must be obtained in another way, and to this end we followed the same procedure used by Deslouis & Tribollet (1985) by considering asymptotic solutions.

Since the velocity modulation is rapidly damped close to the wall at high frequencies the convective terms can be disregarded in the homogeneous part of (13) which becomes:

$$\mathrm{i}\xi h - \frac{\partial^2 h}{\partial \eta^2} = \frac{\eta^2 \exp\left(-\frac{1}{9}\eta^3\right)}{3^{\frac{5}{3}}\Gamma\left(\frac{4}{3}\right)}. \tag{19}$$

Since the frequency is large, the distance over which a concentration wave proceeds is small. Then $\exp\left(-\frac{1}{9}\eta^3\right)$ can be considered as equal to one:

$$h = \lambda(\eta)\int_0^{\eta} \lambda^{-2}(\eta')\left[-\int_0^{\eta'} \frac{\eta''^2 \lambda(\eta'')}{3^{\frac{5}{3}}\Gamma\left(\frac{4}{3}\right)}\mathrm{d}\eta'' + K_1\right]\mathrm{d}\eta' \tag{20}$$

with $$\lambda(\eta) = \exp\{-(\mathrm{i}\xi)^{\frac{1}{2}}\eta\} \quad \text{and } K_1 = \int_0^\infty \frac{\eta''^2\lambda(\eta'')}{3^{\frac{5}{3}}\Gamma(\frac{4}{3})}\mathrm{d}\eta''.$$

Then $$\left.\frac{\mathrm{d}h}{\mathrm{d}\eta}\right|_0 = \frac{2}{3^{\frac{5}{3}}\Gamma(\frac{4}{3})}\frac{1}{(\mathrm{i}\xi)^{\frac{3}{2}}}. \tag{21}$$

This complex function represented in terms of amplitude and phase shift yields

$$\left.\frac{\partial h}{\partial \eta}\right|_0 = \frac{0.359}{\xi^{\frac{3}{2}}}, \quad \arg\left(\left.\frac{\partial h}{\partial \eta}\right|_0\right) = -135°.$$

As mentioned above, this asymptotic behaviour has already been proposed by Fortuna & Hanratty (1971).

The values relative to (21) have also been reported in table 2 for ξ between 7 and 13. It can be concluded that a satisfying overlap exists between values of equation (17) and equation (21) around ξ equal to 13, as shown in figure 2.

4. Frequency response of a microelectrode

From an experimental viewpoint, it must be emphasized that the behaviour shown by (17) and (21) has often been used for characterizing respectively the low-frequency and the high-frequency responses of a real microelectrode. However, the function $\partial h/\partial\eta|_0$ represents only a local value and if one refers now to the frequency $\omega/2\pi$ instead of the local dimensionless frequency ξ, one can expect that at any frequency $\omega/2\pi$, the leading edge of a real microelectrode will always be under a low-frequency regime: indeed the local thickness of the diffusion layer equal to $3^{\frac{2}{3}}\Gamma(\frac{4}{3})\,\delta(x)$, proportional to $x^{\frac{1}{3}}$, is very small at the leading edge and ξ remains there always small even for high $\omega/2\pi$ values; in addition, though the relevant area decreases when $\omega/2\pi$ increases, its contribution to the overall flux is not negligible because the amplitude is constant whereas over the remaining 'high-frequency' area downstream the amplitude is damped as $\xi^{-\frac{3}{2}}$.

Therefore, so as to predict the frequency dependence of a microelectrode, it is necessary to integrate the local flux expression over the whole electrode area.

The local flux is

$$\tilde{j} = Dc_\infty\left[\frac{\bar{\alpha}}{D(x-x_1(z))}\right]^{\frac{1}{3}}\left(\frac{\tilde{\alpha}}{\bar{\alpha}} - \frac{\tilde{\beta}}{\bar{\alpha}}\frac{\mathrm{d}x_1}{\mathrm{d}z}\right)\left.\frac{\partial h}{\partial \eta}\right|_0. \tag{22}$$

For a rectangular probe, the overall flux $\tilde{J}_R$ depends only on $\tilde{\alpha}$, the velocity component in the mean flow direction

$$\tilde{J}_R = Dc_\infty L\left(\frac{\bar{\alpha}l^2}{D}\right)^{\frac{1}{3}}\frac{\tilde{\alpha}}{\bar{\alpha}}H(\sigma'), \tag{23}$$

with $$\sigma' = \omega\left(\frac{l^2}{D\bar{\alpha}^2}\right)^{\frac{1}{3}}, \quad H(\sigma') = \frac{3}{2\sigma'}\int_0^{\sigma'}\left.\frac{\partial h}{\partial \eta}\right|_0 \mathrm{d}\xi.$$

For a circular probe, the overall flux is

$$\tilde{J}_c = \int_{-R}^{R}\mathrm{d}z\int_{R-(R^2-z^2)^{\frac{1}{2}}}^{R+(R^2-z^2)^{\frac{1}{2}}} Dc_\infty\left[\frac{\bar{\alpha}}{D(x-x_1(z))}\right]^{\frac{1}{3}}\frac{\tilde{\alpha}}{\bar{\alpha}}\left.\frac{\partial h}{\partial \eta}\right|_0 \mathrm{d}x, \tag{24}$$

the term containing $\tilde{\beta}$ in (22) makes no contribution because dx_1/dz is an odd function in z.

Then, $\tilde{J}_c$ depends also only on $\tilde{\alpha}$ the velocity component in the mean flow direction.

If one interchanges the order of integration in (24), the analytical form of $\tilde{J}_c$ becomes

$$\tilde{J}_c = c_\infty (\bar{\alpha} D^2 d^5)^{\frac{1}{3}} \frac{\tilde{\alpha}}{\bar{\alpha}} H_x(\sigma), \tag{25}$$

with

$$\sigma = \omega \left(\frac{d^2}{D\bar{\alpha}^2}\right)^{\frac{1}{3}}, \quad H_x(\sigma) = \frac{3}{2\sigma^{\frac{5}{2}}} \int_0^\sigma (\sigma^3 - \xi^3)^{\frac{1}{2}} \left.\frac{\partial h}{\partial \eta}\right|_0 d\xi. \tag{26}$$

The dimensionless functions H_x or H must not be confused with $\mathscr{H}$ (dimensions in Coulombs) defined in (3).

4.1. *Low-frequency solution* (σ or $\sigma' < 13$)

For the range of σ or σ' values considered, any point of the microelectrode area is governed by the low-frequency regime.

In quasi-steady state, σ and σ' tend towards zero, so from (25) and (23):

$$\tilde{J}_c = \tfrac{3}{2} \times 0.84130 \frac{1}{3^{\frac{5}{3}} \Gamma(\frac{4}{3})} c_\infty (\bar{\alpha} D^2 d^5)^{\frac{1}{3}} \frac{\tilde{\alpha}}{\bar{\alpha}},$$

$$\tilde{J}_R = \tfrac{3}{2} \frac{1}{3^{\frac{5}{3}} \Gamma(\frac{4}{3})} D c_\infty L \left(\frac{\bar{\alpha} l^2}{D}\right)^{\frac{1}{3}} \frac{\tilde{\alpha}}{\bar{\alpha}}.$$

We verify, from (6) and (7), that:

$$\frac{\tilde{J}_c}{\tilde{\alpha}} = \frac{1}{3} \frac{\bar{J}_c}{\bar{\alpha}}, \quad \frac{\tilde{J}_R}{\tilde{\alpha}} = \frac{1}{3} \frac{\bar{J}_R}{\bar{\alpha}}.$$

For a rectangular probe, the expression of $H(\sigma')$ is obtained from the series expansion (17) if $\sigma' \leqslant 13$:

$$H(\sigma') = \frac{3}{2} \sum_{m=0}^{m_{max}} \frac{(i\sigma')^m}{m+1} \left.\frac{\partial h_m}{\partial \eta}\right|_0. \tag{27}$$

For a circular probe one has:

$$H_x(\sigma) = \frac{3}{2\sigma^{\frac{5}{2}}} \sum_{m=0}^{m_{max}} \left(\int_0^\sigma (\sigma^3 - \xi^3)^{\frac{1}{2}} (i\xi)^m \, d\xi \left.\frac{\partial h_m}{\partial \eta}\right|_0 \right),$$

and

$$H_x(\sigma) = \frac{3}{2} \sum_{m=0}^{m_{max}} (i\sigma)^m I_m \left.\frac{\partial h_m}{\partial \eta}\right|_0. \tag{28}$$

with

$$I_m = \int_0^1 (1 - x^3)^{\frac{1}{2}} x^m \, dx.$$

The numerical values of I_m are easy to compute. In particular $I_0 = 0.8413$.

The analytical expressions of the frequency response for a rectangular or for a circular probe given by (27) or (28) can be obtained from the coefficients $\partial h_m/\partial \eta|_0$ given in table 1 and m_{max} values given in table 2. They are in good agreement with

$f^+ = \frac{\sigma'}{2\pi}$	σ'	From (27)		From (29) and (31) Nakoryakov *et al.* (1986)		From (36)	
		$A/A(0)$	θ	$A/A(0)$	θ	$A/A(0)$	θ
0	0	1	0	1	0	—	—
0.159	1	0.9729	−15.7	0.9725	−15.7	—	—
0.318	2	0.8973	−30.5	0.8965	−30.7	—	—
0.477	3	0.7889	−43.7	0.7891	−43.8	—	—
0.637	4	0.6688	−54.3	0.6714	−54.2	—	—
0.796	5	0.5570	−61.7	0.5601	−61.6	0.5290	−62.9
0.955	6	0.4670	−66.1	0.4638	−66.4	0.4528	−65.9
1.114	7	0.4019	−68.4	0.3844	−69.10	0.3966	−68.1
1.273	8	0.3561	−69.7	—	—	0.3532	−69.9
1.432	9	0.3221	−70.9	—	—	0.3187	−71.3
1.592	10	0.2943	−72.1	—	—	0.2905	−72.5
1.751	11	0.2705	−73.2	—	—	0.2671	−73.5
1.910	12	0.2497	−73.9	—	—	0.2472	−74.4
2.069	13	0.2313	−73.3	—	—	0.2302	−75.1
2.228	14	—	—	—	—	0.2154	−75.8
2.387	15	—	—	—	—	0.2024	−76.3

TABLE 3. Amplitude and phase shift of function $H(\sigma')$ on a rectangular microelectrode. A good overlap is found between (27) and (36) for $6 \leqslant \sigma' \leqslant 13$

the expression given by Nakoryakov *et al.* (1986) and obtained by a fitting technique from the numerical integration:

for σ and $\sigma' \leqslant 6$:

$$\frac{|H(\sigma')|}{|H(0)|} = (1 + 0.056\sigma'^2 + 0.00126\sigma'^4)^{-\frac{1}{2}}, \tag{29}$$

$$\frac{|H_x(\sigma)|}{|H_x(0)|} = (1 + 0.049\sigma^2 + 0.0006\sigma^4)^{-\frac{1}{2}}, \tag{30}$$

and

$$\arg H = -\arctan[0.276\sigma'(1 + 0.02\sigma'^2 - 0.00026\sigma'^4)], \tag{31}$$

$$\arg H_x = -\arctan[0.242\sigma(1 + 0.0124\sigma^2 - 0.00015\sigma^4)]. \tag{32}$$

The different expressions are compared in table 3 for amplitude and phase shift for the rectangular microelectrode.

The result in (31) is in disagreement with the low-frequency expression given by Fortuna & Hanratty (1971) (e.g. the argument according to our notation is $\arg H = -\arctan[0.61\sigma']$) and recalled by Talbot & Steinert (1987), but is in good agreement with the numerical integration given by Mao & Hanratty (1985).

4.2. *High-frequency solution*

If σ' is larger than 13, the integration of (29) relative to the rectangular probe must be split into two parts since the trailing portion of the microelectrode is characterized by the high-frequency behaviour:

$$H(\sigma') = \frac{3}{2\sigma'}\left[\int_0^{\sigma_1} \left.\frac{\partial h}{\partial \eta}\right|_0 \mathrm{d}\xi + \int_{\sigma_1}^{\sigma'} \left.\frac{\partial h}{\partial \eta}\right|_0 \mathrm{d}\xi\right]. \tag{33}$$

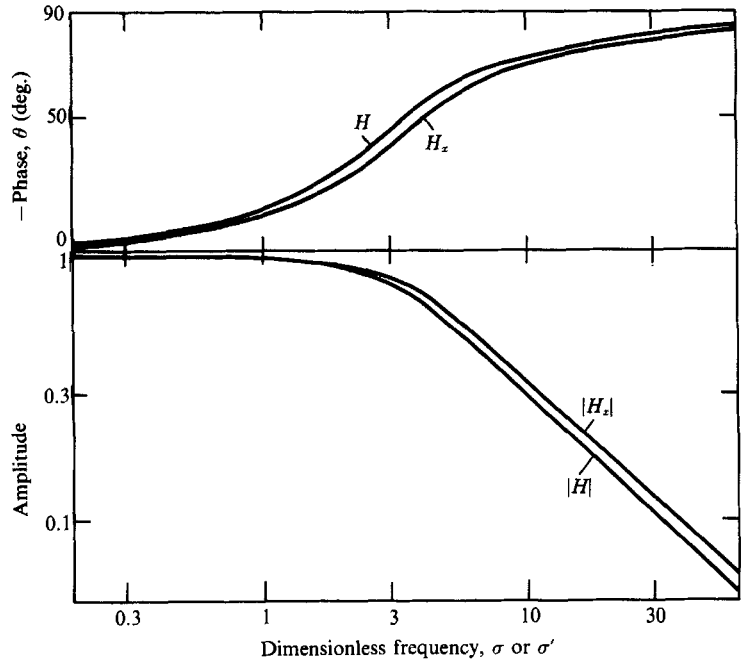

FIGURE 3. Dimensionless transfer functions for the rectangular (H) or circular (H_x) microelectrodes *vs.* σ or σ'.

The first integral corresponds to a low-frequency range and the second one to the high-frequency range where expressions (17) and (21) must be used respectively. We get

$$H(\sigma') = \frac{1}{\sigma'} B(\sigma'_1) - \frac{2}{3^{\frac{5}{3}}\Gamma(\frac{4}{3})} \frac{1}{(\mathrm{i}\sigma')^{\frac{3}{2}}}, \tag{34}$$

where

$$B(\sigma'_1) = \frac{3}{2}\left[\sum_{m=0}^{m_{\max}} \frac{\mathrm{i}^m \sigma_1'^{m+1}}{m+1} \left.\frac{\partial h_m}{\partial \eta}\right|_0 + \frac{4}{3^{\frac{5}{3}}\Gamma(\frac{4}{3})\,\mathrm{i}^{\frac{3}{2}}\sigma_1'^{\frac{1}{2}}}\right]. \tag{35}$$

$B(\sigma'_1)$ has been calculated for $\sigma'_1 \leqslant 13$ and $B(\sigma'_1)$ is constant in the frequency range $6 \leqslant \sigma'_1 \leqslant 13 : B(\sigma'_1) = -\mathrm{i}$. This result means that (33) is valid for $\sigma' \geqslant 6$ and therefore can be written as:

$$\frac{H(\sigma')}{H(0)} = \frac{3.715}{\mathrm{i}\sigma'} - \frac{3.99}{(\mathrm{i}\sigma')^{\frac{3}{2}}}. \tag{36}$$

As a consequence, a fair overlap between (27) and (36) is obtained for $6 \leqslant \sigma' \leqslant 13$ (see table 3).

Equation (36) is identical to that given by Nakoryakov *et al.* (1986) and obtained by a fitting procedure from the $H(\sigma')$ variation determined by a numerical integration.

By using the same splitting, the expression of the transfer function for a circular probe can be written as

$$H_x(\sigma) = \frac{3}{2\sigma^{\frac{5}{2}}}\left(\sum_{m=0}^{m_{\max}}\left(\int_0^{\sigma_1} (\sigma^3 - \xi^3)^{\frac{1}{2}} (\mathrm{i}\xi)^m \,\mathrm{d}\xi\right)\left.\frac{\partial h_m}{\partial \eta}\right|_0 + \frac{2}{3^{\frac{5}{3}}\Gamma(\frac{4}{3})}\int_{\sigma_1}^{\sigma} (\sigma^3 - \xi^3)^{\frac{1}{3}} \frac{\mathrm{d}\xi}{(\mathrm{i}\xi)^{\frac{8}{3}}}\right). \tag{37}$$

In (37), the part depending on σ_1 cannot be explicitly separated as in (34). However, the numerical integration shows that $H_x(\sigma)$ is independent of σ_1 for

$6 \leqslant \sigma_1 \leqslant 13$ and is in good agreement with the expression obtained by Nakoryakov *et al.* (1986):

$$\frac{H_x(\sigma)}{H_x(0)} = \frac{4.416}{\mathrm{i}\sigma} - \frac{5.3}{(\mathrm{i}\sigma)^{\frac{3}{2}}}. \tag{38}$$

Therefore, from (38) and (36), the amplitude at high frequencies varies as σ^{-1}, and the limiting phase is equal to $-90°$.

On figure 3, the variations of $H(\sigma')$ and $H_x(\sigma)$ in amplitude and phase shift are plotted versus the dimensionless frequencies. In the first approximation, the two curves are shifted by a constant factor. In fact, considering (31) and (32) at low frequency, this factor is equal to 1.14. It tends to 1.18 at high frequency according to (38) and (36). In the low-frequency range, Fortuna & Hanratty (1971) had already justified this fact by showing that a circular microelectrode of diameter d yields the same current as a rectangular one of length $0.82d$ and width d and therefore the factor 1.14 is consistent with $0.82^{-\frac{2}{3}}$.

5. Experimental results

A well-defined periodic flow is very difficult to obtain in a pipe or a channel, and the previous attempts with those flows (e.g. Ambari *et al.* 1986; Fortuna & Hanratty 1971; Talbot & Steinert 1987) were not completely successful.

As mentioned by Ambari *et al.* (1986), the flow generated by a rotating disk, the angular velocity of which is sinusoidally modulated, is accurately known for both amplitude and phase. In this earlier work, only the experimental variation of the amplitude was reported. But the probe geometry (diameter and radial eccentricity) was such that the cutoff frequency of H_x was high and therefore the main observed effect was due to the hydrodynamic transfer function between the disk angular velocity and the fluid velocity.

In the present work, we mounted a circular microelectrode embedded in an insulating rotating disk with the following characteristics, diameter $d = 0.03$ cm and distance of its centre to the rotation axis $r = 1.1$ cm, allowing observing for the best conditions the effects anticipated in the theoretical analysis.

A fast electrochemical redox reaction provides a simple means of generating a controlled mass flux between the solution and the wall where the concentration of one ionic species can be set equal to zero.

For example the elementary reduction step $\mathrm{Ox} + \mathrm{ne}^- \rightarrow \mathrm{Red}$ corresponds to a current I which reaches a maximum value at large negative potentials imposed on the microelectrode such that the concentration of the oxidized species at the electrode becomes zero.

The electrode behaves then as a perfect mass sink and the current I is proportional to the mass flux J as:

$$I = nFJ,$$

where F is the Faraday number.

The flux itself is related to the concentration gradient by the Fick's law

$$J = D \left.\frac{\partial c}{\partial y}\right|_0.$$

In the present case, we selected a fast redox system (ferri/ferrocyanide) in its reduction step

$$Fe(CN)_6^{3-} + e^- \rightarrow \mathrm{Fe(CN)}_6^{4-}$$

at equimolar concentrations (10^{-2} M).

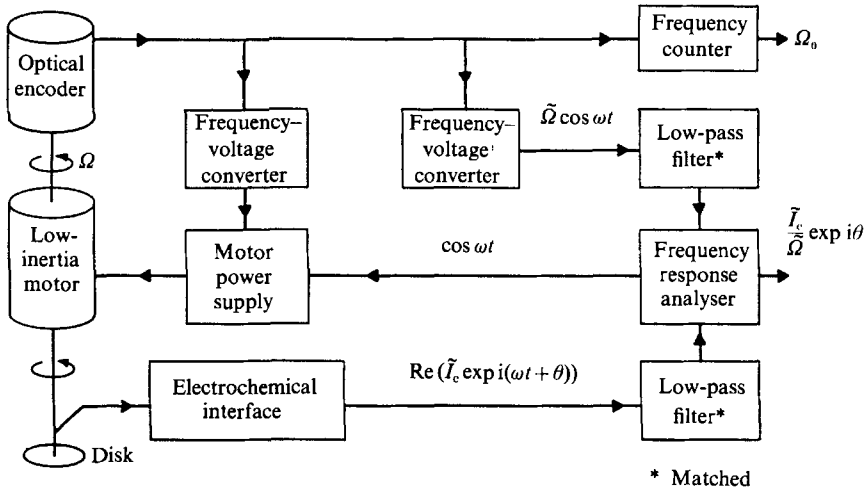

FIGURE 4. Experimental set-up.

KCl was used as supporting electrolyte for minimizing the transport of ferricyanide ions by migration due to the electric field. The material used for the microelectrode was platinum.

The experiments were carried out in a cylindrical cell with a sufficient volume (≈ 1 l) for ensuring the conditions at infinity required by the rotating-disk theory as defined by Kármán (1921) or Cochran (1934).

The experimental device is described in figure 4. The rotating disk electrode is driven by a very low-inertia d.c. motor, the angular velocity of which is controlled by a servo system accurately ensuring a prescribed value $\bar{\Omega}$, and a small sine wave modulation is superimposed at a frequency ω with a frequency response analyser (FRA Solartron 1172) such that the instantaneous velocity is:

$$\Omega(t) = \Omega(1 + (\tilde{\Omega}/\bar{\Omega})\cos\omega t).$$

Here $(\tilde{\Omega}/\bar{\Omega})$ is not larger than 0.1 to fulfil the linearity conditions.

An optical encoder is fastened by a rigid coupling to the motor and delivers a train of pulses which are fed to a frequency to voltage converter. At its output, a sine wave voltage, proportional to $\tilde{\Omega}\cos\omega t$, is sent to the X input of the FRA. The instantaneous response of the diffusion current $I(t)$ is picked up on a rotating mercury contactor in electrical contact with the electrode.

The fluctuating component of the current $\mathrm{Re}(\tilde{I}_c \exp i(\omega t+\theta))$ is sent to the input Y of the FRA. The measured transfer function is obtained as $\tilde{I}_c/\tilde{\Omega}$.

This quantity is related to the electrohydrodynamical (EHD) impedance Z_{EHD} otherwise defined in electrochemical studies (see for instance Deslouis *et al.* 1982; Tribollet & Newman 1983).

With the symbols of this work, one has:

$$Z_{EHD} = \frac{\tilde{I}_c}{\tilde{\Omega}} = \frac{1}{3}\frac{\bar{I}_c}{\bar{\alpha}}\frac{\tilde{\alpha}}{\tilde{\Omega}}\frac{H_x(\sigma)}{H_x(0)} = \mathscr{H}\frac{\tilde{\alpha}}{\tilde{\Omega}}. \tag{39}$$

The motor characteristics enable a modulation frequency $\omega/2\pi$ of 100 Hz for an average angular velocity Ω_0 of 600 r.p.m. to be reached.

The hydrodynamic transfer function $\tilde{\alpha}/\tilde{\Omega}$ had been calculated by Ambari *et al.*

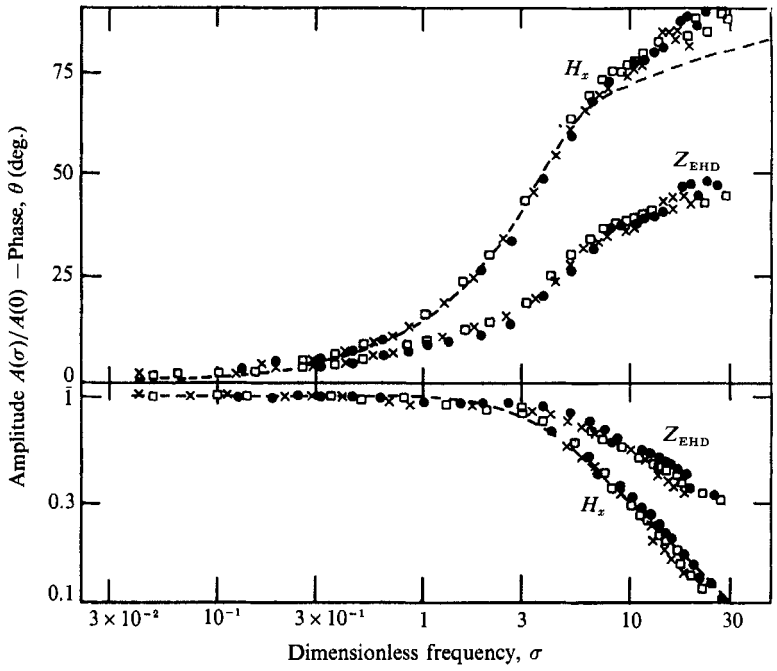

FIGURE 5. Experimental response of a platinum circular microelectrode ($d = 0.03$ cm, $r = 1.1$ cm) on a rotating disk. Solution KCl M, $Fe(CN)_6^{3-/4-}$ 10^{-3} M, $\theta = 25°$. ●, 120; □, 150; ×, 180 r.p.m.

(1986) from the integration of the unsteady Navier–Stokes equations given by Tribollet & Newman (1983).

In the high-frequency range, this function $\tilde{\alpha}/\tilde{\Omega}$ is increasing as the square root of the frequency, a situation which is specific to the rotating disk system because the velocity perturbation is diffusing from the wall towards the bulk.

As a consequence, the condition $\tilde{\alpha}/\bar{\alpha} \ll 1$ valid in the low-frequency range, is not necessarily verified at high frequencies if the modulation level $\tilde{\Omega}$ is kept constant and thus, the quadratic term $\tilde{\alpha}(\partial\tilde{c}/\partial x)$, neglected in (11), would play a role and induce a nonlinearity.

We therefore chose the modulation level $\tilde{\Omega}$ experimentally such that the linearity was fulfilled at any frequency. Anyhow, in turbulence measurements, this problem is pointless since the situation is reversed, i.e. the velocity perturbations are transported from the bulk to the wall and $\tilde{\alpha}$ is then expected to decrease when the frequency increases.

In figure 5, we have plotted the experimental variation of $Z_{EHD}(\sigma)$ and that of $H_x(\sigma)$ deduced by applying expression (39) in amplitude and phase shift θ. On the same figure we recall, as a dashed line, the theoretical variation of $H_x(\sigma)$ from expressions (28) and (38). The agreement is excellent for the amplitude, but for the phase shift a small discrepancy appears in the high-frequency range: the experimental phase shift seems to tend faster towards the asymptotic value of $-90°$.

It is known, from the work of Ling (1963), that the term describing molecular diffusion in the x-direction, which appears in the steady-state equation, is negligible provided that the dimensionless parameter $\bar{\alpha}l^2/D > 5000$; if a probe fulfils this condition, one must expect the same condition to apply in the low-frequency range.

Conversely, in the high-frequency range of flow modulation, only a small area close to the leading edge of the microelectrode corresponds to the low-frequency regime but, as previously mentioned, its influence becomes predominant and the effect of $\partial^2 c/\partial x^2$ is maximum for small values of x and y. However, this reason may not be sufficient to explain the discrepancy at high frequency if we consider that the argument of Ling is still valid at high frequency. Another reason for the discrepancy could be found in the influence of the convection term in the z-direction when the frequency increases. Indeed, for the rotating disk system at low frequency, the mean velocity vector and the fluctuating one are aligned and therefore no z velocity component (in the local reference frame) exists. At high frequency, the fluctuating velocity component tends to be aligned with the circumferential direction and, hence, a z velocity component appears. In these conditions, we may expect an influence of $\tilde{\beta}$ in the response, because the argument put forward previously about the absence of its contribution (see (22)) concerned a perfectly circular sensor, and is unlikely to be accurate for a real one.

For the major part of the hydrodynamical applications involving p.s.d. measurements, the knowledge of the magnitude of $H_x(\sigma)$ is sufficient, in order to apply (2) and the expressions (28) and (38) can be used. For most of the pulsatile flows studied so far, the frequency domain is smaller than in turbulence studies, mainly because it is difficult to perform mechanical modulations at high frequencies. Therefore, the amplitude and phase shift, which are both useful in this instance, can be accurately predicted since the agreement between theory and experiment is excellent in the respective frequency domains of interest (i.e. for $\sigma < 8$).

In conclusion, this work contributes to the idea that electrochemical probes can be very useful for hydrodynamic studies involving instabilities or periodic flows. Although the mass transfer process causes a damping at lower frequencies than, for example, thermal probes, the transfer function is now accurately known and can be used to correct the damping.

In particular, the results of the combined analytical and numerical calculations of this transfer function presented here were experimentally verified by use of a rotating disk system for which a periodic flow can be properly determined.

The results also point to the fact that the apparent discrepancies observed among the different exponent values of frequency reported in the literature in the high-frequency range come from the usual implicit but incorrect argument that one can apply the expression established for a local transfer function (i.e. h) to a real microelectrode, however small.

The authors express their thanks to Dr P. Mitschka (Institut of Chem. Process Func. Czech. Acad. of Sciences, Prague) for helpful suggestions.

REFERENCES

AMBARI, A., DESLOUIS, C. & TRIBOLLET, B. 1986 Frequency response of the mass transfer rate in a modulated flow at electrochemical probes. *Intl J. Heat Mass Transfer* **29**, 35.

BOGOLYUBOV, YU. YE., GESHEV, P. I., NAKORYAKOV, V. Y. & OGORODNIKOV, I. A. 1972 Theory of electrodiffusion method applied to the characteristic spectra measurement in turbulent flow. *Prikl. Mekh. Teckln. Fiz.* **4**, 112.

COCHRAN, W. G. 1934 The flow due to a rotating disk. *Proc. Camb. Phil. Soc.* **30**, 365.

DESLOUIS, C., EPELBOIN, I., GABRIELLI, C. & TRIBOLLET, B. 1977 Impédance électromécanique obtenue au courant limite de diffusion à partir d'une modulation sinusoïdale de la vitesse de rotation d'une électrode à disque. *J. Electroanal. Chem.* **82**, 251.

DESLOUIS, C., GABRIELLI, C., SAINTE-ROSE FANCHINE, PH. & TRIBOLLET, B. 1982 Electrohydrodynamical impedance on a rotating disk electrode. I. Redox system. *J. Electrochem. Soc.* **129**, 107.

DESLOUIS, C. & TRIBOLLET, B. 1985 Mass transfer for a modulated flow at a rotating disk electrode; asymptotic solutions. *J. Electroanal. Chem.* **185**, 171.

DESLOUIS, C., TRIBOLLET, B. & VIET, L. 1983 The correlation between momentum and mass transfer for a turbulent or periodic flow in a circular pipe by electrochemical methods. *4th Intl Conference on Physicochemical Hydrodynamics, Ann. NY Acad. Sci.* **404**, 471.

DUMAINE, J. Y. 1981 Etude numérique de la réponse en fréquence des sondes électrochimiques. *Lett. Heat Mass Transfer* **8** (4), 293.

FORTUNA, G. & HANRATTY, T. J. 1971 Frequency response of the boundary layer on wall transfer probes. *Intl J. Heat Mass Transfer* **14**, 1499.

KÁRMÁN, TH. VON 1921 Uber Laminare und turbulente Reibung. *Z. angew. Math. Mech.* **1**, 233.

LEVEQUE, M. A. 1928 Transmission de chaleur par convection. *Ann. Mines* **13**, 283.

LING, S. C. 1963 Heat transfer from a small isothermal span wise strip on an insulated boundary. *Trans. ASME* C: *J. Heat Transfer* **85**, 230.

MAO, Z. X. & HANRATTY, T. J. 1985 The use of scalar transport probes to measure wall shear stress in a flow with imposed oscillations. *Expt Fluids* **3**, 129.

MOLLET, L., DUMARGUE, P., DAGUENET, M. & BODIOT, D. 1974 Calcul du flux limite de diffusion sur une microélectrode de section circulaire – Equivalence avec une électrode de section rectangulaire – Vérification expérimentale dans le cas du disque tournant en régime laminaire. *Electrochimica Acta* **19**, 841.

NAKORYAKOV, V. E., BUDUKOV, A. P., KASHINSKY, O. N. & GESHEV, P. I. 1986 *Electrodiffusion Method of Investigation into the Local Structure of Turbulent Flows* (ed. V. G. Gasenko). Novosibirsk.

NAKORYAKOV, V. E., KASHINSKY, O. N. & KOZMENKO, B. K. 1983 Electrochemical method for measuring turbulent characteristics of gas–liquid flows. *Measuring techniques in Gas–Liquid Two Phase Flows, IUTAM Symposium, Nancy, France*, pp. 695–721.

NEWMAN, J. 1968 Numerical solution of coupled, ordinary, differential equations. *Ind. Engng Chem.* **7**, 514.

NEWMAN, J. 1973 *Electrochemical Systems*. Prentice Hall.

PATEL, R. D., MCFEELY, J. J. & JOLLS, K. R. 1975 Wall mass transfer in laminar pulsatile flow in a tube. *AIChE J.* **21**, 259.

PEDLEY, T. J. 1972 On the forced heat transfer from a hot film embedded in the wall in two-dimensional unsteady flow. *J. Fluid Mech.* **55**, 329.

TALBOT, L. & STEINERT, J. J. 1987 The frequency response of electrochemical wall shear probes in pulsatile flow. *Trans. ASME* K: *J. Biomech. Engng* **109**, 60.

TOKUDA, K., BRUCKENSTEIN, S. & MILLER, B. 1975 The frequency response of limiting currents to sinusoidal speed modulation at a rotating disk electrode. *J. Electrochem. Soc.* **122**, 1316.

TRIBOLLET, B. & NEWMAN, J. 1983 The modulated flow at a rotating disk electrode. *J. Electrochem. Soc.* **130**, 2016.

VOROTYNTSEV, M. A., MARTEM'YANOV, S. A. & GRAFOV, B. M. 1984 Temporal correlation of current pulsations at one or several electrodes: A technique to study hydrodynamic fluctuation characteristics of a turbulent flow. *J. Electroanal. Chem.* **179**, 1.